GEMINI NEAR-INFRARED SPECTROSCOPY OF LUMINOUS z ~ 6 QUASARS:

CHEMICAL ABUNDANCES, BLACK HOLE MASSES AND Mg II ABSORPTION

Linhua Jiang et al.

2007 September

Presented by Emily McLinden

November 9, 2007

Motivation for study

Luminous, high-redshift quasars are:

- “direct probes of the early universe when the first generations of galaxies and quasars formed.”

- “essential for studying the accretion history of BHs, galaxy formation, and chemical evolution at very early epochs.”

Background info for HRSLQs

- Central BH masses of 10^9 - 10^{10} $M_\odot$
- HRSLQs emit near the Eddington limit
  -indicates rapid growth of central BH
- Solar or supersolar metallicity
  -determined from emission-line ratios
  -indication of “vigorous star formation and element enrichment in 1st Gyr”

Investigating High-Redshift Luminous Quasars

The study by Jiang et al. seeks to:

- Obtain and fit spectra of the quasars
  -rest-frame UV emission shifted to NIR- contains strong emission lines
  -provides info about “physical conditions and emission mechanisms of the BLR

- Use Mg II emission lines to determine the redshifts of the quasars

- Detect and fit other individual emission lines in each quasar

- Determine emission-line ratios
  -measure gas metallicity in the quasar
  -track metallicity/ abundances with redshift
  -high metallicity can confirm vigorous star formation and element enrichment

- Estimate masses of the central BHs
  -understand growth of the central BHs and accretion rates for quasars in the early universe

- Search for Mg II absorption systems in quasar spectra
  -strong Mg II absorption --> usually galaxy halos or disks
  -analyze if number density of systems evolves with increasing redshift

Meet the Quasars

- Six quasars discovered by SDSS, chosen from a paper by Fan et al.
- 5 quasars observed on Gemini South GNIRS, 1 quasar observed on Gemini North NIRI
- All have extensive follow up in x-ray, Spitzer, millimeter/submillimeter, and radio
- High S/N Gemini data
- Excellent NIR coverage from Gemini

TABLE 1

Log of Observations

Quasar (SDSS)	Redshift	z_{AB} (mag)	J (mag)	Date	Instrument	t_{exp} (minutes)
J083643.85+005453.3	5.82	18.74 ± 0.05	17.89 ± 0.05	2006 Feb 19	GNIRS	70
J103027.10+052455.0	6.28	20.05 ± 0.10	18.87 ± 0.10	2006 Mar 20, 26	GNIRS	140
J104433.04−012502.2	5.80	19.23 ± 0.07	18.31 ± 0.10	2006 Mar 28	GNIRS	120
J130608.26+035626.3	5.99	19.47 ± 0.05	18.77 ± 0.10	2006 Mar 26, 27	GNIRS	140
J141111.29+121737.4	5.93	19.66 ± 0.08	18.95 ± 0.05	2006 Mar 28	GNIRS	120
J162331.81+311200.5	6.22	20.09 ± 0.10	19.15 ± 0.10	2004 Aug 15, 2004 Sep 14, 2005 Aug 22, 24	NIRI (K)	180

Notes.—Redshifts, z_{AB} (AB magnitudes), and J (Vega-based magnitudes) are from the quasar discovery papers of Fan et al. (2000, 2001, 2004).

The Data

Spectra in this study have better S/N than previous studies

- GNIRS observations of 5 quasars covered wavelengths of 0.9 - 2.5 μm
- K-band spectrum for single quasar on NIRI, coverage from 1.9 - 2.35 μm
- Sufficient resolution/minimum dispersion to separate Mg II λλ2796, 2803 doublet
- A or F spectroscopic standard star observed for flux calibration and telluric correction

- Both sets of data reduced using IRAF
- Flat-fielding, distortion correction, wavelength calibration --> frames combined to extract 1-D spectra
- Spectra were flux calibrated and telluric correction applied from standard stars
- Different order spectra scaled to form a single spectrum
- GNIRS spectra calibrated to J-band magnitude, NIRI data scaled to J magnitude assuming a power-law continuum slope of $\alpha_\nu = -0.5 (f_\nu \sim \nu^{\alpha_\nu})$

Spectra from GNIRS

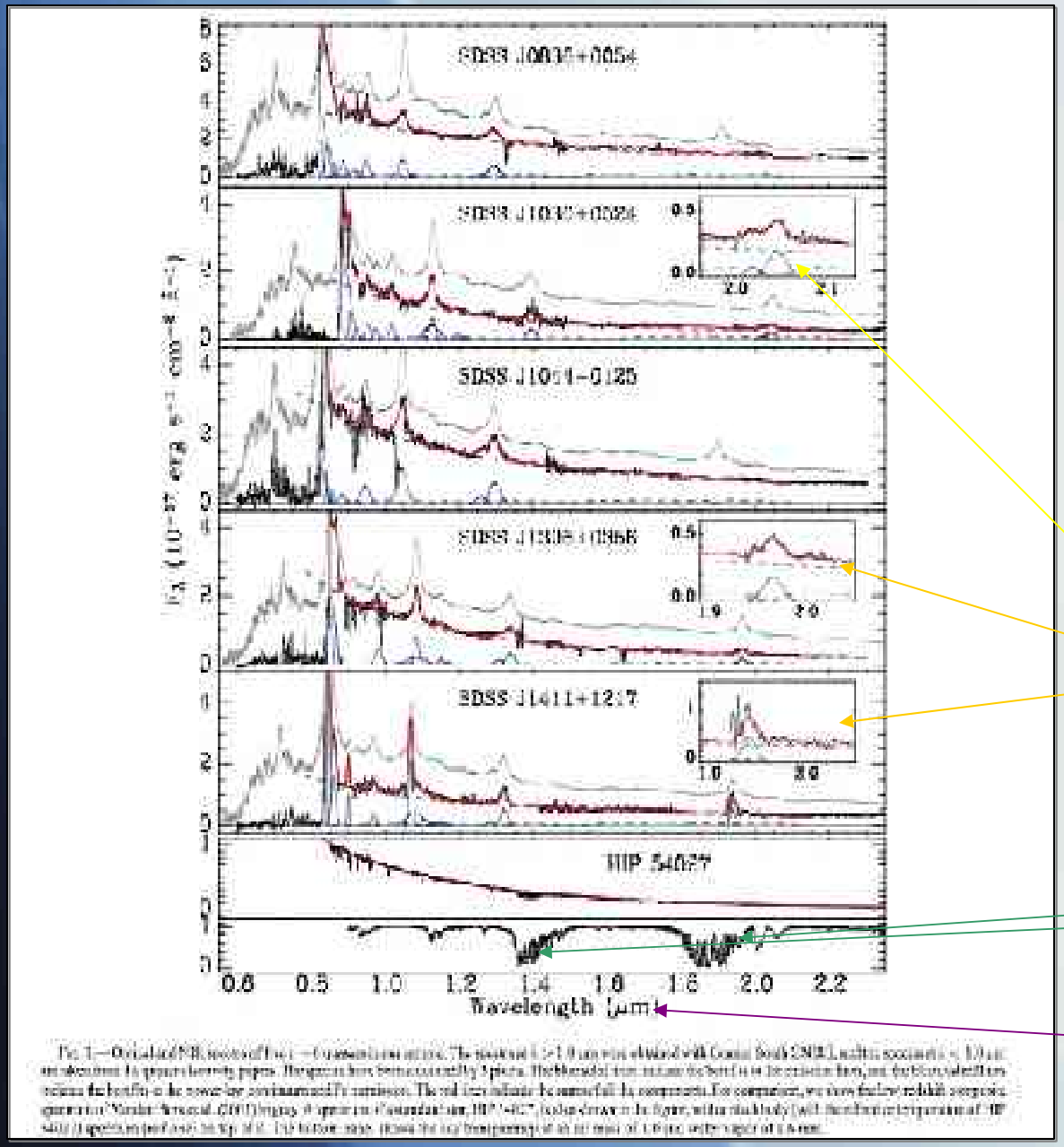

Spectra from NIRI

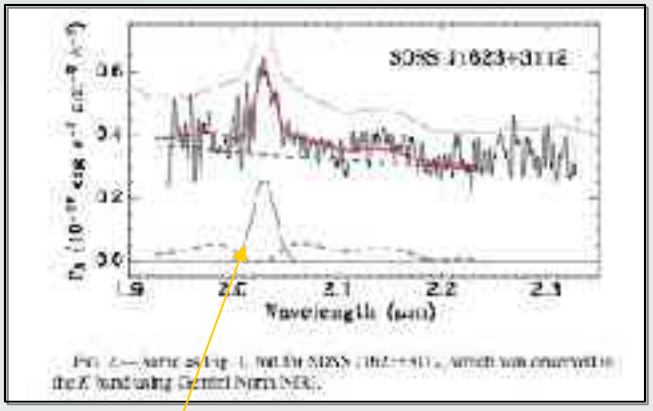

Mg II emission used for redshift estimates

Strong telluric absorption

Redshifted wavelengths

Spectral Fit and Emission-Line Measurements

- 1st have to fit and subtract UV Fe II emission

  -contaminates most of the UV-optical region, blends w/ other lines in the spectrum
- Done using a power-law fit to the continuum emission and a model fit to the Fe II emission - repeat until left with smooth, featureless spectrum
- Mg II lines used to determine redshifts

TABLE 2

REDSHIFTS AND CONTINUUM SLOPES

Quasar (SDSS) (1)	Redshift (2)	$Slope_{UV}(\alpha_\nu)^a$ (3)	$Slope_{opt}(\alpha_\nu)^b$ (4)
J0836+0054	5.810 ± 0.003^c	-0.62 ± 0.06	-0.52
J1030+0524	6.309 ± 0.009	$0.46^{+0.18}_{-0.35}$	-0.31
J1044−0125	5.778 ± 0.005^c	$-0.27^{+0.09}_{-0.10}$	-0.30
J1306+0356	6.016 ± 0.003	$0.50^{+0.12}_{-0.14}$	-0.12
J1411+1217	5.927 ± 0.004	$-0.21^{+0.18}_{-0.19}$	-0.51
J1623+3112	6.247 ± 0.003		-0.32

[a] UV continuum slopes measured from the Gemini spectra.
[b] Optical continuum slopes taken from Jiang et al. (2006).
[c] Taken from Kurk et al. (2007).
[d] Measured from the C III] λ1909 emission line.

- Mg II emission line has only a small blueshift - more reliable than C IV and others lines to measure the redshift
- Measured redshifts in good agreement with other papers
- SDSS J0836+0054 and SDSS J1044-0125 observed in high humidity - No Mg II line detected - Redshifts taken from Kurk et al. (2007) and measured from the CIII λ1909 line, respectively

Spectral Fit and Emission-Line Measurements Continued

Other emission lines (if detected) were also fit after subtraction of Fe II and power-law continuum:

TABLE 3

EMISSION-LINE PROPERTIES

Line	Quantity	J0836+0054	J1030+0524	J1044−0125	J1306+0356	J1411+1217	J1623+3112
N v	EW	15.9 ± 0.7	4.9 ± 0.1	3.9 ± 0.2	9.3 ± 0.3	28.9 ± 0.4	...
	FWHM	31.5 ± 1.0	8.7 ± 0.2	10.4 ± 0.3	15.0 ± 0.2	22.3 ± 0.3	...
Si II	EW	3.6 ± 0.5	3.0 ± 0.2	2.3 ± 0.1	1.7 ± 0.1	0.9 ± 0.1	...
	FWHM	15.0 ± 0.6	15.8 ± 0.7	12.7 ± 0.3	12.8 ± 0.4	3.7 ± 0.3	...
O I	EW	7.4 ± 0.1	6.7 ± 0.3	2.6 ± 0.2	...	6.7 ± 0.2	...
	FWHM	24.6 ± 0.5	18.8 ± 0.7	24.3 ± 1.3	...	8.1 ± 0.3	...
C II	EW	5.8 ± 0.5	4.0 ± 0.4	...	...	...	...
	FWHM	41.9 ± 3.1	17.0 ± 1.5	...	...	...	...
Si IV	EW	9.3 ± 4.2	8.5 ± 1.7	8.9 ± 0.7	9.5 ± 0.8	8.1 ± 6.4	...
	FWHM	25.3 ± 5.9	18.4 ± 2.9	35.7 ± 1.8	29.0 ± 2.0	21.5 ± 12.2	...
C IV	EW	15.0 ± 1.6	40.0 ± 3.1	24.7 ± 2.1	29.6 ± 2.4	36.2 ± 5.8	...
	FWHM	37.1 ± 3.0	27.3 ± 2.9	42.2 ± 3.1	26.5 ± 2.1	17.5 ± 1.6	...
He II	EW	...	3.4 ± 2.0	...	2.6 ± 1.8	5.1 ± 2.5	...
	FWHM	...	21.7 ± 6.8	...	15.5 ± 7.5	39.0 ± 25.6	...
O III]	EW	...	2.3 ± 1.3	...	2.7 ± 2.0	2.5 ± 2.5	...
	FWHM	...	22.9 ± 11.0	...	26.9 ± 19.4	42.2 ± 34.0	...
Al III	EW	1.8 ± 0.9	...	5.0 ± 1.6	7.0 ± 3.1	5.1 ± 2.3	...
	FWHM	16.3 ± 6.8	...	31.0 ± 6.7	34.5 ± 14.7	25.6 ± 9.2	...
C III]	EW	18.9 ± 2.3	19.3 ± 2.8	24.0 ± 1.8	19.1 ± 3.9	26.1 ± 3.2	...
	FWHM	53.2 ± 6.9	31.6 ± 3.3	50.3 ± 3.2	37.6 ± 7.4	31.3 ± 2.6	...
Mg II	EW	...	46.1 ± 3.7	...	24.9 ± 2.1	37.5 ± 3.5	27.4 ± 3.9
	FWHM	...	35.8 ± 2.2	...	33.2 ± 2.2	23.7 ± 2.7	34.4 ± 2.4

NOTE.—Rest-frame FWHM and EW are in units of Å.

Emission-Line Ratios

- Ratios used to measure gas metallicity in the quasars
- Can track chemical evolution with redshift
- Different elements form on different time scales

  - C, O, Mg from explosions of massive stars --> rapid enrichment

  -N is 2nd generation element --> slow enrichment

  -He is primordial element --> abundance changes little with time

TABLE 4

FLUX RATIOS

Ratio	J0836+0054	J1030+0524	J1044−0125	J1306−0356	J1411+1217	J1623−3112
N v/C iv	.44 ± 0.17	0.21 ± 0.02	0.23 ± 0.03	0.55 ± 0.05	0.56 ± 0.04	...
Si iv/C iv	0.32 ± 0.04	0.12 ± 0.02	0.13 ± 0.02	0.10 ± 0.01	0.02 ± 0.01	...
O i/C iv	0.62 ± 0.07	0.26 ± 0.02	0.14 ± 0.02	...	0.12 ± 0.02	...
C ii/C iv	0.47 ± 0.06	0.14 ± 0.02	...	...	...	...
Si ii/C iv	0.72 ± 0.33	0.27 ± 0.06	0.43 ± 0.05	0.41 ± 0.05	0.13 ± 0.10	...
He ii/C iv	...	0.07 ± 0.04	...	0.08 ± 0.05	0.06 ± 0.05	...
O iii]/C iv	...	0.05 ± 0.03	...	0.08 ± 0.06	0.03 ± 0.02	...
Al iii/C iv	0.10 ± 0.05	...	0.15 ± 0.05	0.15 ± 0.07	0.05 ± 0.02	...
C iii]/C iv	0.95 ± 0.15	0.29 ± 0.05	0.68 ± 0.08	0.38 ± 0.08	0.24 ± 0.03	...
Fe ii/Mg ii	...	5.45 ± 0.58	...	5.77 ± 0.72	5.27 ± 0.72	3.21 ± 0.62

Emission-Line Ratios Continued

- Emission-Line flux ratios are normalized to the C IV fluxes
- Emission-line ratios from quasars in the range $2.0 \leq z \leq 4.0$ and $-29.5 \leq M_B \leq -24.5$ are taken from Nagao et al. (2006) for comparison.
- Figure shows that most flux ratios don't exhibit strong evolution up to $z \sim 6$.
- Some trend towards higher CII/C IV and OI/CIV ratios with increasing redshift.

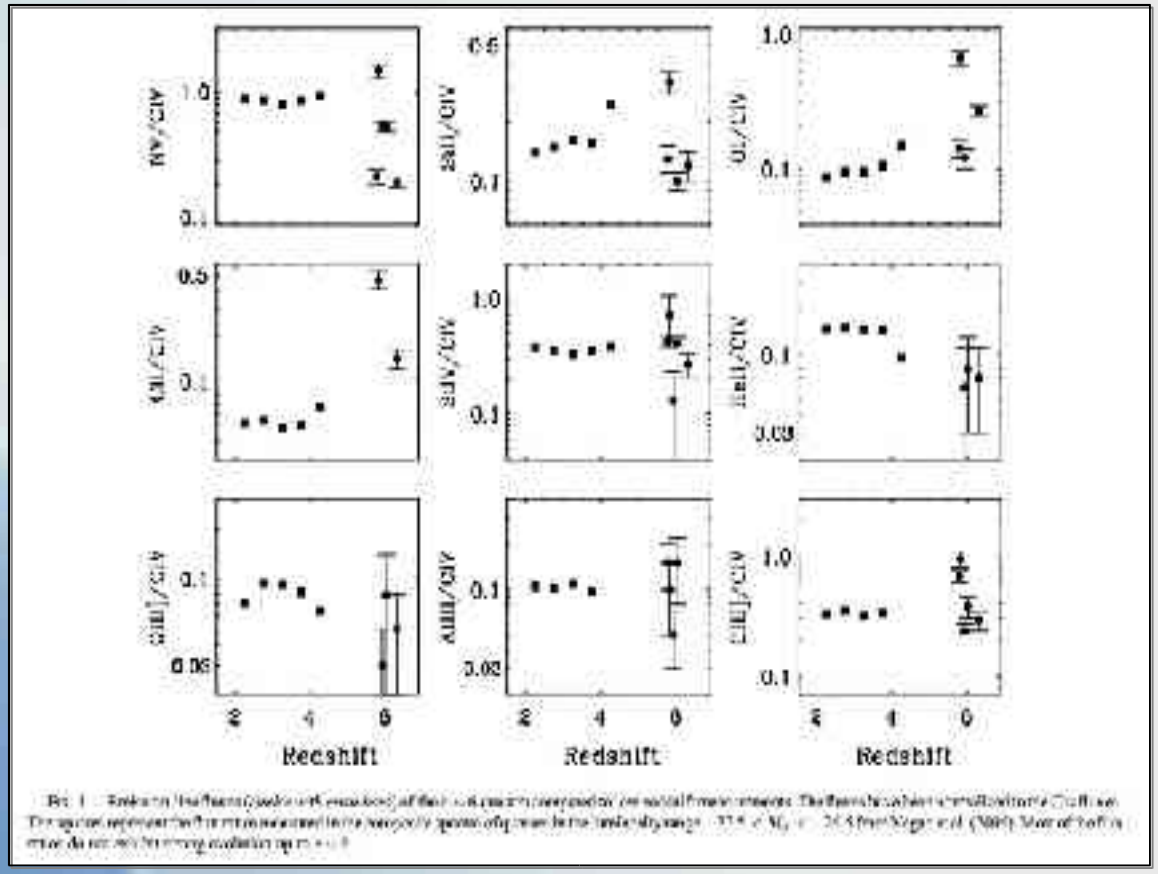

Estimating Gas Metallicity from Emission- Line Ratios

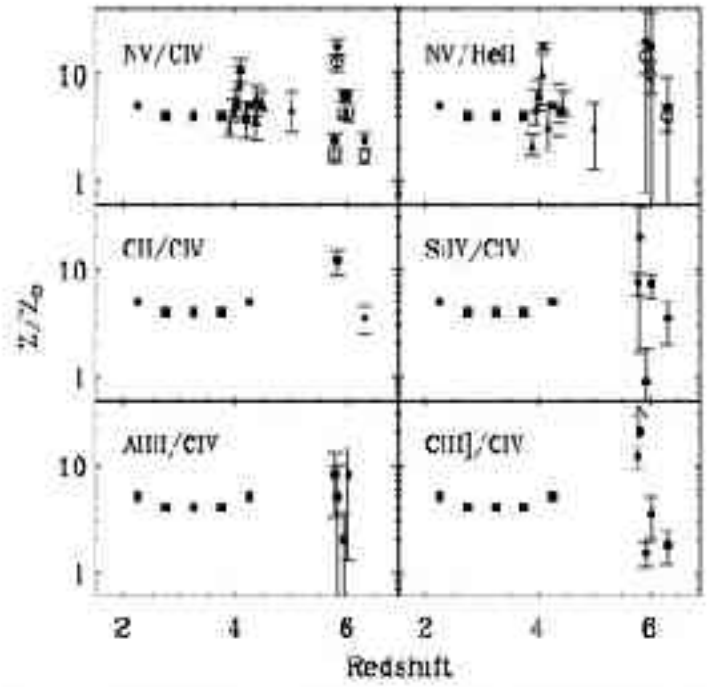

FIG. 4.—Chemical abundances of quasars derived from line ratios as a function of redshift. The open circles represent the metallicities derived from the N V/C IV and N V/He II ratios using Fig. 5 of Hamann et al. (2002). The filled circles represent the metallicities derived from the line ratios using Fig. 29 of Nagao et al. (2006). The squares show the averaged metallicities of quasars for the luminosity range $-28.5 < M_B < -25.5$ from Nagao et al. (2006). The triangles show the metallicities of $11.3.9 < z < 5.0$ quasars from Dietrich et al. (2003a). The metallicities estimated from each line ratio show no strong evolution up to $z > 6$ within the errors.

- Photoionization models show that emission-line ratios can be used to estimate gas metallicity of quasars
- Use methods of Hamann et al. (2002) and Nagao et al. (2006) to estimate metallicity from various ratios as functions of redshift
- Abundances are scaled to latest solar abundances (Baldwin et al., 2003)
- Metallicity is supersolar (typically ~ 4 $Z_{\odot}$)
- Figure shows no strong evolution of metallicity up to z ~ 6

Fe II / Mg II Ratio

- Important for understanding chemical evolution at HRS
- Fe in solar neighborhood from Sne Ia --> enrichment only on a timescale of 1 Gyr after initial starburst
- Production of elements like Mg dominated by Sne of types II, Ib, and Ic --> enrichment can occur very soon after initial burst
- Therefore Fe/Mg ratio puts “useful constraint on the age and chemical enrichment of the as in the quasar enrichment of the gas”
- For quasars in this study, Fe II/ Mg II ratios were derived with typical values of 4.9 ± 1.4
- Lack of strong evolution in Fe II/ Mg II abundance continues to z ~ 6.

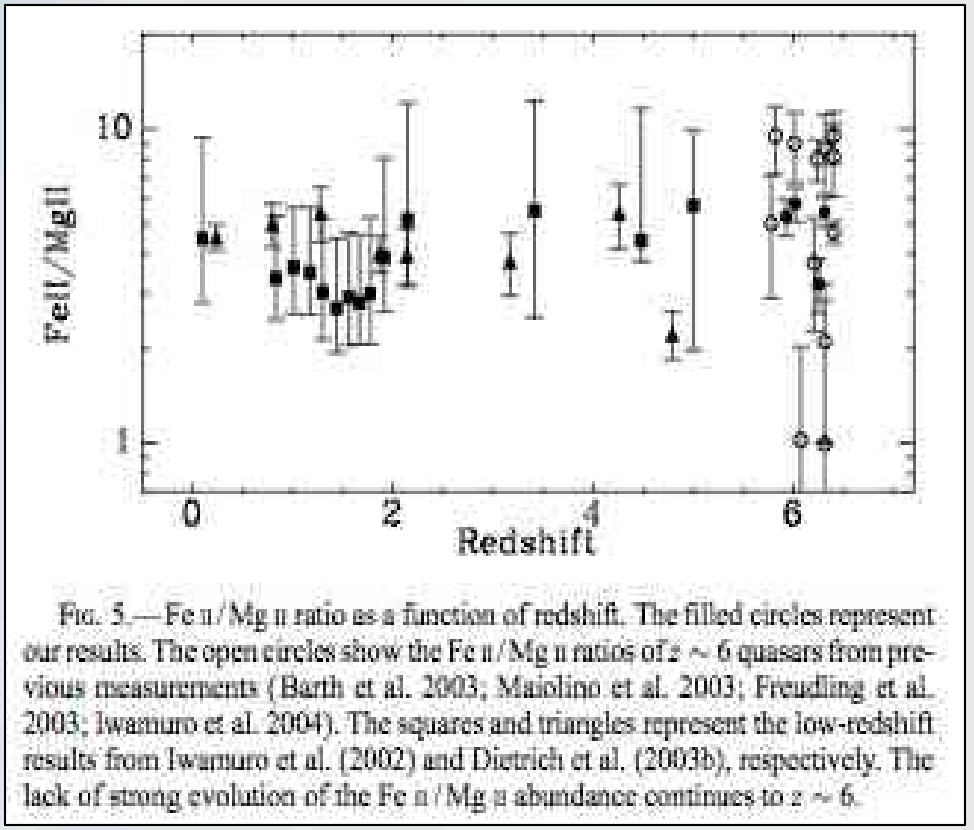

FIG. 5.—Fe II / Mg II ratio as a function of redshift. The filled circles represent our results. The open circles show the Fe II / Mg II ratios of $z \sim 6$ quasars from previous measurements (Barth et al. 2003; Maiolino et al. 2003; Freudling et al. 2003; Iwamuro et al. 2004). The squares and triangles represent the low-redshift results from Iwamuro et al. (2002) and Dietrich et al. (2003b), respectively. The lack of strong evolution of the Fe II / Mg II abundance continues to $z \sim 6$.

Results are compared to HRS results from Barth et al., Maiolino et al., Freudling et al., and Iwamuro et al. and LRS results from Iwamuro et al. (2002) and Dietrich et al. (2003)

Central BH Masses

- Want to estimate BH masses of HRSLQs to understand growth of BHs and accretion rates for quasars in the early universe
- BH masses can be derived from broad line emission line widths and continuum luminosities
- In this study BH masses are estimated using equations derived by Vestergaard & Peterson (2006) and McLure & Dunlop (2004):

$$M_{BH}(\text{C IV}) = 4.57 \left(\frac{\text{FWHM(C IV)}}{\text{Km s}^{-1}} \right)^2 \left(\frac{\lambda L_\lambda (1350\ \text{Å})}{10^{44}\ \text{ergs s}^{-1}} \right)^{0.53}$$

$$M_{BH}(\text{Mg II}) = 3.2 \left(\frac{\text{FWHM(Mg II)}}{\text{Km s}^{-1}} \right)^2 \left(\frac{\lambda L_\lambda (3000\ \text{Å})}{10^{44}\ \text{ergs s}^{-1}} \right)^{0.62}$$

Central BH Masses continued

TABLE 3
CENTRAL BH MASSES

Quasar (SDSS) (1)	L_{bol}[a] (2)	L_{bol}/L_{Edd}[b] (3)	M_{BH} (C IV) (4)	M_{BH} (Mg II) (5)	M'_{BH} (Mg II)[c] 6
J083[illegible]0054	47.32	0.44	9.2 ± 1.6	...	
J1010+0858	47.87	0.29	3.6 ± 0.9	1.9 ± 0.2	2.1 ± 0.4
J1044−0125	47.63	0.2[illegible]	10.5 ± 1.6	...	
J1306+0356	47.93	0.6[illegible]	2.2 ± 0.6	1.1 ± 0.1	2.2 ± 0.3
J14[illegible]+12[illegible]	47.23	0.04	[illegible].3 ± 0.2	3.9 ± 0.1	0.9 ± 0.2
J1623+21[illegible]	47.33	1.1[illegible]	...	1.5 ± 0.3	

NOTE.—All masses are given in $10^8\ M_\odot$.
[a] Bolometric luminosity in $\log(\mathrm{erg\ s^{-1}})$. Turn Hang et al. (2008).
[b] L_{bol} is derived from M_{BH} (C IV) except for SDSS J1623+3112, whose L_{bol} is derived from M_{BH} (Mg II).
[c] M'_{BH} is estimated from the same relation by M. Vestergaard et al. (2007, in preparation).

- Results in good agreement w/ Kurk et al (2007).
- Additional estimate made using latest derivation for Mg II by Vestergaard --> agrees with this study's C IV estimates
- Similar to other HRSLQs that have BH masses of 10^9 - $10^{10}\ M_\odot$

Central BH Masses continued

- This means billion-solar-mass BHs formed in < 1Gyr after big bang!!
- How could this happen?

seed black holes from Pop III stars, assume M ~ 10^2- 10^4 $M_\odot$

accretion at the Eddington rate gives mass at time t as $M(t) = M_0 e^{t/\tau}$ where $\tau = 4.5 \times 10^8$, is radiative efficiency

start with $M_0 = 10^3 M_\odot$ at z = 20 --> $\tau = 4.5 \times 10^7$ = e-folding time --->15 e-foldings to go from z= 20 to z=6

--> $e^{t/\tau} = 3.3 \times 10^6$ --> then result is BH mass $M_t = 3.3 \times 10^9 M_\odot$

if quasar shines at only 1/2 of Eddington limit --> only 7.5 e-foldings to go from z = 20 to z= 6 --> $e^{t/\tau} = 2000$

--> hard to form BH with masses of 10^9- 10^{10} $M_\odot$ in first Gyr

"if Eddington-limited accretion is via standard thin disks, BHs are likely to be spun up and the radiative efficiency and Eddigton time sxale will increase"

- Therefore super-Eddington accretion or lower radiative efficiency needed to form BHs of observed size by z = 6!

Eddington rate - mass accretion rate for which a BH with = 0.1 has Eddington Luminosity

Eddington luminosity - largest value of L that still allows material to fall inward

Mg Absorption systems at z < 6

- Looked for Mg II λλ2796, 2803 absorption systems in 5 of the 6 spectra
- Looked for Mg II absorbers with rest equivalent width > 1.5 A for z > 3 and absorbers with rest equivalent width > 1 A at z < 3

  -these systems can be detected to 7 σ significance at lowest S/N portions of the spectra
- First search for lines w/ separations matching Mg II λλ2796, 2803 doublet

  -->then look for other emission lines in these systems
- 5 systems are found --> redshift and rest-frame Ews are determined

Mg Absorption systems at z < 6 continued

TABLE 6
Absorber Lines

Absorption System	λ_{obs} (Å)	ID	z_{abs}	W_λ (Å)
SDSS J0836+0054	13761.81	Mg II (2796)	3.7479	2.56
	13795.63	Mg II (2803)	3.7424	2.36
SDSS J1306+0356 (a)	9952.30	Mg II (2796)	2.2913	1.36
	9977.30	Mg II (2803)	2.2902	1.36
	9137.13	Mg I (2852)	2.2028	1.26
SDSS J1306+0356 (b)	9977.58	Mg II (2796)	2.1393	3.76
	9999.77	Mg II (2803)	2.1384	3.83
	9186.23	Fe II (2600)	2.5335	1.34
SDSS J1306+0356 (c)	15806.55	Mg II (2796)	4.6468	2.32
	15847.97	Mg II (2803)	...	...
	9795.54	Al II (1670)	4.8652	1.11
	15232.21	Fe II (2600)	4.8638	1.46
SDSS J1306+0356 (d)	15446.35	Mg II (2796)	...	...
	15491.06	Mg II (2803)	4.8826	2.31
	9822.49	Al II (1670)	4.8795	0.78
	15299.94	Fe II (2600)	4.8819	1.95

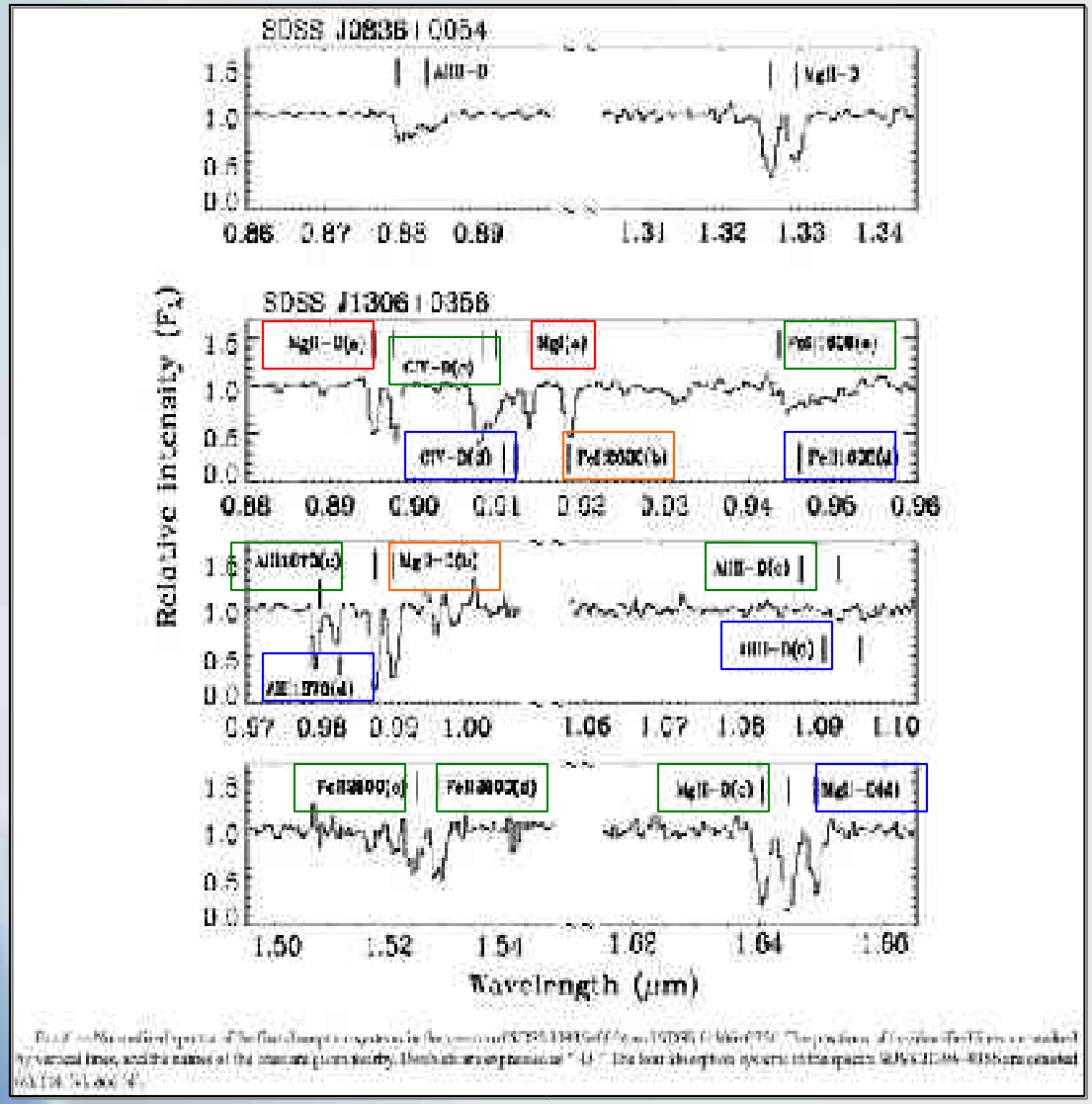

Mg II absorbers continued
Determining number density of absorber systems

$$dN/dz = \frac{N_a}{\Sigma\, \Delta Z\, (EW^{2796})_i}$$

Where $\Sigma\, \Delta Z\, (EW^{2796})$ is the redshift path covered by a spectrum

- The two derived data points from this study
- Other data points from Mg II absorbers at low redshift from Nestor et al., and Prochter et al.
- Previous studies indicate density doesn't evolve with redshift, but density of strongest absorbers does increase with redshift
- This study indicates no evolution up to z ~ 4…but too small a sample to rule it out and too much uncertainty…. Results inconclusive….NEED MORE SAMPLES!

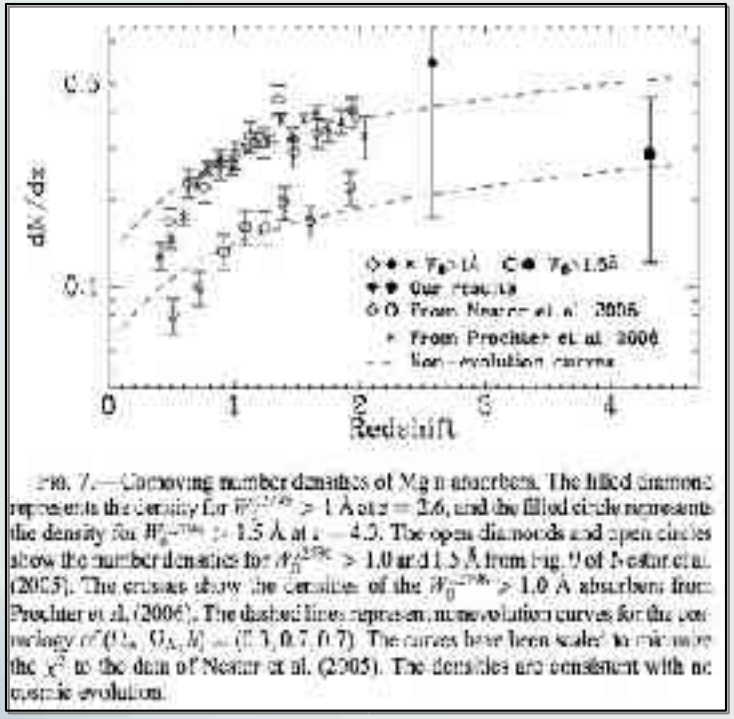

FIG. 7.—Comoving number densities of Mg II absorbers. The filled diamond represents the density for $W_0^{2796} > 1$ Å at $z = 2.6$, and the filled circle represents the density for $W_0^{2796} > 1.5$ Å at $z = 4.2$. The open diamonds and open circles show the number densities for $W_0^{2796} > 1.0$ and 1.5 Å from Fig. 9 of Nestor et al. (2005). The crosses show the densities of the $W_0^{2796} > 1.0$ Å absorbers from Prochter et al. (2006). The dashed lines represent no-evolution curves for the cosmology of $(\Omega_m, \Omega_\Lambda, h) = (0.3, 0.7, 0.7)$. The curves have been scaled to minimize the χ^2 to the data of Nestor et al. (2005). The densities are consistent with no cosmic evolution.

CONCLUSIONS

- Flux ratios determined for detected emission lines --> ratios do not show strong evolution with redshift
- Gas metallicity determined from emission-line ratios --> metallicity found to be supersolar --> no strong evolution of metallicity up to z ~ 6
- Fe II/ Mg II estimated --> estimates match low-redshift samples
- These investigations indicate vigorous star formation and element enrichment occurred in the 1st Gyr after the big bang

- Central BH masses determined from C IV and Mg II emission lines
- Results are in good agreement with other z ~ 6 quasars

- Five intervening Mg II absorption systems were found --> the absorbers at 4.8668 and 4.8823 are the most distant absorbers to date --> small sample seems to confirm no evolution, but more data needed